Shaping site-controlled uniform arrays of SiGe/Si(001) islands by in situ annealing

J. J. Zhang' , A. Rastelli' , H. Groiss, J. Tersoff, F. Schäffler, O. G. Schmidt, and G. Bauer

Citation: Appl. Phys. Lett. **95**, 183102 (2009); doi: 10.1063/1.3258648
View online: http://dx.doi.org/10.1063/1.3258648
View Table of Contents: http://aip.scitation.org/toc/apl/95/18
Published by the American Institute of Physics

Shaping site-controlled uniform arrays of SiGe/Si(001) islands by *in situ* annealing

J. J. Zhang,[1,a)] A. Rastelli,[2,a)] H. Groiss,[1] J. Tersoff,[3] F. Schäffler,[1] O. G. Schmidt,[2] and G. Bauer[1]
[1]*Institute of Semiconductor and Solid State Physics, University Linz, A-4040 Linz, Austria*
[2]*Institute for Integrative Nanosciences, IFW Dresden, Helmholtzstr. 20, D-01069 Dresden, Germany*
[3]*IBM Research Division, T. J. Watson Research Center, Yorktown Heights, New York 10598, USA*

(Received 27 August 2009; accepted 14 October 2009; published online 3 November 2009)

We investigate the effect of *in situ* annealing on the shape, size, and chemical composition of ordered SiGe islands grown on pit-patterned Si(001) substrates. In contrast to planar substrates, intermixing with substrate material occurs symmetrically during annealing because the substrate patterning pins the island position and suppresses lateral motion. The results are consistent with surface-mediated intermixing and demonstrate that annealing is an effective method to tune the island properties with no appreciable deterioration of the ensemble homogeneity. © *2009 American Institute of Physics*. [doi:10.1063/1.3258648]

The Ge/Si(100) system is a prototype for investigating fundamental properties of heteroepitaxial growth.[1,2] After completion of an initial pseudomorphic wetting layer, three-dimensional (3D) islands form. At relatively high substrate temperatures, growing islands evolve from unfaceted prepyramids to pyramids, domes, and eventually barns[3] before plastic relaxation occurs.[1] During *in situ* postgrowth annealing islands with steep facets transform back to shallower pyramids[4–6] as they intermix with Si from the substrate. This intermixing occurs via lateral island motion, which is driven by surface-mediated alloying.[5–7] Additionally, island coarsening takes place, which leads to a drop in island density and a broadening of the island size distribution.[4–6,8] For possible applications in electronic devices, ordered island arrays are generally required.[9–11] Ge growth on pit-patterned Si substrates is an established approach to obtain islands which are not only spatially ordered but also morphologically homogeneous.[12–14] The presence of relatively deep pits appears to suppress the island coarsening that typically occurs for growth on planar Si substrates.[13,14] It is therefore interesting to study the influence of the pits on the island evolution during annealing and to test whether annealing can be used to tailor the properties of site-controlled islands.

In this letter, we investigate the postgrowth annealing of ordered SiGe islands grown on pit-patterned substrates. We observe that after 20 min of *in situ* annealing, barn-shaped islands are transformed into pyramid-shaped islands and the island size homogeneity is preserved. We determine the chemical composition profiles of the annealed SiGe islands by a nanotomography technique, which is based on atomic force microscopy (AFM) and selective wet chemical etching.[15] During etching, ring-shaped depressions are observed on the surface of partially etched islands. Cross-section transmission electron microscopy (TEM) data show that the "ring" can be ascribed to the interface between the original as-grown island and the intermixed SiGe region developed during annealing. During annealing on planar substrates, lateral islands motion causes dramatically asymmetric intermixing.[5] In contrast, here no lateral island motion is observed, and the intermixing is highly symmetric. The observations can be explained by assuming that intermixing and consequent shape changes are mainly due to surface diffusion and, most importantly, that the islands are constrained to their original positions by the patterned pits.

Two-dimensional pit arrays with a period of 400 nm were patterned by holographic lithography and reactive ion etching. After *ex situ* chemical cleaning, the samples were dipped in a diluted hydrofluoric acid solution to create a hydrogen terminated surface before loading to the solid source molecular beam epitaxy (MBE) system. After *in situ* outgassing and 36 nm Si buffer growth, 20 ML Ge were deposited at 720 °C at a rate of 0.03 Å/s and then the sample was kept at 720 °C for 20 min before cooling to room temperature (RT). The annealed sample was etched at RT in NHH solution [1:1 vol. (28% NH_4OH):(31% H_2O_2)], which selectively etches $Si_{1-x}Ge_x$ alloys over pure Si and shows an etching rate increasing approximately exponentially with the Ge fraction x, no preferential etching direction, and a negligible dependence on strain.[16] The surface morphology was investigated using AFM in tapping mode at RT.

Figure 1 shows AFM images of samples obtained after deposition of 20 ML Ge at 720 °C [Fig. 1(a)] and after subsequent *in situ* annealing for 20 min [Fig. 1(b)]. After the deposition of 20 ML Ge at 720 °C, a well-ordered array of barn-shaped islands is observed. After 20 min of *in situ* annealing, the barns have transformed into pyramids, as demonstrated by the surface orientation maps[17] in the insets of Figs. 1(a) and 1(b). In such plots, the spots associated with the steep facets typical for barns [see circles in the inset of Fig. 1(a)] disappear in favor of large {105} facets [circle in the inset of Fig. 1(b)]. The histograms in Figs. 1(c) and 1(d) display the island height distribution before and after *in situ* annealing. Annealing reduces substantially the average height $\langle H \rangle$ of the islands. However the relative width of the size distribution, quantified by the standard deviation σ, does not change much (values are quoted in the figures). The shape change and height reduction reflect the redistribution of material during intermixing, as previously reported for islands on planar substrates.[4–6] However, on planar substrates, annealing also leads to coarsening, i.e., shrinkage of

a)Authors to whom correspondence should be addressed. Electronic addresses: jianjun.zhang@jku.at and rastelli@ifw-dresden.de.

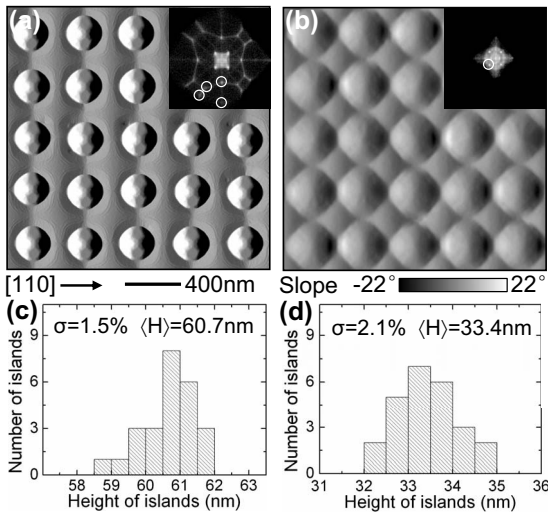

FIG. 1. AFM images of islands obtained by deposition of 20 ML Ge at 720 °C on a pit-patterned Si(001) substrate with a period of 400 nm (a) and of islands grown with same nominal parameters followed by *in situ* annealing at 720 °C for 20 min (b). The grayscale represents the first derivative along the horizontal axis. The insets show surface orientation maps with circles marking the steep barn facets in (a) and shallow {105} facets in (b). The corresponding histograms of island height distribution are shown in (c) and (d), respectively. Average height values ⟨*H*⟩ and relative standard deviation σ of the distributions are quoted.

smaller islands in favor of larger islands. Coarsening is expected whenever islands with significantly different sizes are able to exchange material.[7,8] The presence of periodically distributed pits creates islands with very similar sizes in a symmetric environment.[12–14] Therefore the driving force for coarsening is extremely small, so coarsening is effectively suppressed and the size homogeneity is well preserved.

The question now is: how does intermixing take place on the patterned substrates? Figure 2 shows AFM images of the annealed sample prior to etching (a) and after 60 (b), 150 (c), and 500 (d) min wet chemical etching in NHH. All AFM images were taken at the same sample area. From the etching results, we can see that for most of the islands the SiGe has been etched away symmetrically, indicating that intermixing occurs in a symmetric fashion. In contrast, on planar substrates the intermixing takes place asymmetrically in conjunction with lateral island motion, which is self-sustaining once triggered by small composition fluctuations or environmental asymmetries.[5–7] The image in Fig. 2(d), taken after almost complete removal of the SiGe material, shows no trace of the "half-moon" shaped Si structures that occur

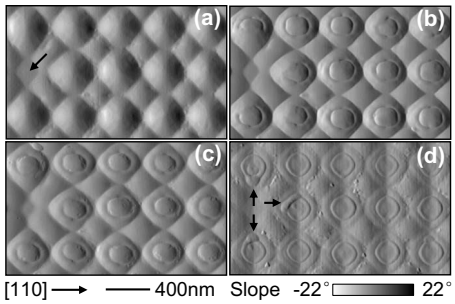

FIG. 2. Sequence of AFM images of the same surface area of the annealed sample prior to wet chemical etching (a) and after 60 min (b), 150 min (c), and 500 min (d), wet chemical etching in NHH. The arrow in (a) marks an unoccupied site of the pattern. Arrows in (d) mark residual Si-rich material after almost complete SiGe etching.

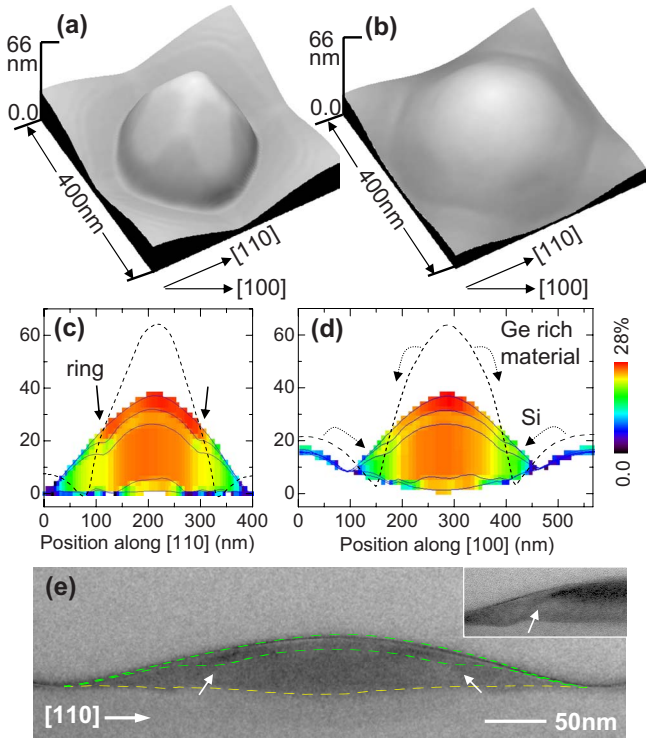

FIG. 3. (Color online) 3D AFM images of representative islands after deposition of 20 ML Ge at 720 °C (a) and after subsequent *in situ* annealing (b). Cross-section through the center of an annealed island, showing Ge distributions obtained from the linescans shown as solid lines along [110] (c) and [100] (d) directions. Linescans of an as-grown island are included as dashed lines for comparison. (e) Bright field cross-sectional TEM images of an annealed island. Some of the AFM linescans from (c) are superimposed in (e) (dashed green lines), along with a linescan (dashed yellow line) obtained after complete SiGe removal in BPA solution. The inset shows the interface region at higher magnification. Arrows in (c) and (e) mark the positions of the rings seen in Fig. 2(b), while arrows in (d) illustrate the material transfer occurring during annealing.

when there is lateral island motion.[5,6] We conclude that pits effectively "pin" the island position, because the center of the pit is an energetically favorable site.[18–20] A similar behavior was previously observed for annealing of closely spaced vertically stacked islands, where the local energy minimum is provided by the tensile strain above buried islands.[6]

On the other hand, islands in an asymmetric environment due to fabrication imperfections [see, e.g., empty site marked in Fig. 2(a)] show a slightly asymmetric shape after annealing. The composition profiles are also asymmetric: the regions of the islands close to the empty site are etched less than the other regions, i.e., they are richer in Si [see Fig. 2(b) and residual material pointed at by arrows in Fig. 2(d)]. It is natural that a strongly asymmetric environment would break the symmetry of the intermixing to some extent. However, even for these islands no evidence of lateral motion is seen.

An interesting feature observed in Figs. 2(b) and 2(c) is a ring-shaped depression on the surface of partially etched islands. What is the origin of these rings? Figures 3(a) and 3(b) display 3D AFM images of unit cells (400×400 nm^2) of the as-grown sample and the sample after annealing, respectively. After annealing, the island base widens to cover nearly the whole pit and the island height decreases. Simultaneously, surrounding Si is incorporated into the island and the Si surface level drops correspondingly. Figures 3(c) and 3(d) show cross sections of the Ge distributions on $(1\bar{1}0)$ and

(010) planes passing through the center of an annealed island, respectively. The AFM linescans taken at different etching times (0, 60, 150, 420, and 500 min) in NHH solution which were used to evaluate the composition are also shown. The kinks in the linescans [see arrows in Fig. 3(c)] reflect local variations in the etching rate—faster at the island center and slower at the island boundary, which means a Ge-rich core and Si-rich shell around the base. We ascribe the Ge-rich core to the original as-grown island and the Si-rich shell to the alloyed SiGe region which develops during annealing. This interpretation is supported by the comparison between the linescans of islands after annealing and etching and linescans of an as-grown island, which are shown by dashed lines in Figs. 3(c) and 3(d). Although the relative vertical offset of the two sets of linescans is somewhat arbitrary, it is reasonable to assume that rings correspond to the interface between the original surface of the as-grown island and the strongly alloyed shell. We have confirmed this scenario using cross-sectional TEM. Figure 3(e) shows a bright field TEM image, and its inset shows a higher magnification image featuring the interface. Only the electrons from the (000) spot were used and the sample was tilted slightly away from the zone axis to minimize the diffraction contrast and thus the strain contrast. The main contrast of the image is the mass-thickness contrast, i.e., dark areas contain heavier atoms or are thicker. The AFM linescans obtained prior to etching and after 150 min etching in NHH solution are superimposed on the TEM image (dashed green lines). Additionally an AFM linescan obtained after complete removal of the SiGe layer by 2 min etching in BPA solution[5] is displayed as a dashed yellow line. The latter represents the interface between the island and the Si substrate, as indicated by the good agreement with the abrupt contrast change seen in the TEM image. Furthermore, in correspondence with the position of the ring [see arrows in Fig. 3(e) and inset], we can see a subtle change in contrast in the TEM image, which we can interpret as the boundary between the original Ge-rich island and the Ge-poor shell forming during annealing.

We can now provide a comprehensive picture of the evolution of islands upon annealing, with reference to Fig. 3(d). Before annealing, islands are generally characterized by a Ge distribution such that the Ge content decreases from the island top toward the base.[21,22] Annealing causes additional Si–Ge intermixing driven by entropy increase, and also by strain energy reduction.[5,7,23] Although some bulklike diffusion may occur during annealing,[24] a dilute alloy can be efficiently obtained by surface diffusion if Si from the surrounding area mixes with Ge taken from the island surface and the mixture is deposited somewhere else, leaving uncovered Ge available for further mixing. From an energetic point of view, taking Ge away from the island top and depositing on the sides together with Si from the surrounding areas seems the most natural path. This lowers the surface area and surface energy, providing the flatter aspect ratio favored by more dilute SiGe,[4] while leaving the most Ge-rich region exposed for further mixing. This pathway is fully consistent with our observations [see arrows in Fig. 3(d)]. The island height decreases as material is removed, and the island base broadens as the diluted mixture accumulates in a Si-rich shell bounded by extended {105} facets. This shell explains the ringlike depression in our etching experiments: the remainder of the original island is richer in Ge, so it etches faster than the surrounding shell. On planar substrates, material is removed from one side of the island and the diluted mixture is deposited on the other side. However, such lateral motion in unfavorable on the patterned substrate, where the pit effectively pins the island position.

In conclusion, we have investigated the effect of *in situ* annealing on the structural properties of ordered SiGe islands on Si(001) pit-patterned substrates. During annealing, islands change shape and alloy with Si. However, in contrast to annealing performed on planar substrates, neither island coarsening nor lateral island motion is observed for islands in the pits. We observe a symmetric intermixing which we mainly ascribe to the presence of pits, which prevent island motion. Only where the environment of an island is asymmetric, alloying is slightly asymmetric. The presence of pits allows one to engineer the shape and composition of islands with annealing without losing the control on their position as well as on ensemble homogeneity.

This work was supported by the EC D-DOTFET Project No. 012150, by the DFG (Grant No. FOR730), and by the GMe and FWF (Grant No. SFB025) in Vienna. The authors acknowledge F. Pezzoli, M. Stoffel, and G. Katsaros for fruitful discussions and D. Pachinger for MBE assistance.

[1] A. Rastelli, M. Stoffel, U. Denker, T. Merdzhanova, and O. G. Schmidt, Phys. Status Solidi A **203**, 3506 (2006), and references therein.
[2] J. Drucker, IEEE J. Quantum Electron. **38**, 975 (2002).
[3] E. Sutter, P. Sutter, and J. E. Bernard, Appl. Phys. Lett. **84**, 2262 (2004).
[4] T. I. Kamins, G. Medeiros-Ribeiro, D. A. A. Ohlberg, and R. Stanley Williams, J. Appl. Phys. **85**, 1159 (1999).
[5] U. Denker, A. Rastelli, M. Stoffel, J. Tersoff, G. Katsaros, G. Costantini, K. Kern, N. Y. Jin-Phillipp, D. E. Jesson, and O. G. Schmidt, Phys. Rev. Lett. **94**, 216103 (2005).
[6] M. Stoffel, A. Rastelli, S. Kiravittaya, and O. G. Schmidt, Phys. Rev. B **72**, 205411 (2005).
[7] Y. Tu and J. Tersoff, Phys. Rev. Lett. **98**, 096103 (2007).
[8] F. M. Ross, J. Tersoff, and R. M. Tromp, Phys. Rev. Lett. **80**, 984 (1998).
[9] *Lateral Alignment of Epitaxial Quantum Dots*, edited by O. G. Schmidt (Springer, Berlin, 2007).
[10] O. G. Schmidt and K. Eberl, IEEE Trans. Electron Devices **48**, 1175 (2001).
[11] S. Fregonese, Y. Zhuang, and J. N. Burghartz, IEEE Trans. Electron Devices **54**, 2321 (2007).
[12] Z. Zhong and G. Bauer, Appl. Phys. Lett. **84**, 1922 (2004).
[13] J. J. Zhang, M. Stoffel, A. Rastelli, O. G. Schmidt, V. Jovanović, L. K. Nanver, and G. Bauer, Appl. Phys. Lett. **91**, 173115 (2007).
[14] C. Dais, G. Mussler, H. Sigg, E. Müller, H. H. Solak, and D. Grützmacher, J. Appl. Phys. **105**, 122405 (2009).
[15] A. Rastelli, M. Stoffel, A. Malachias, T. Merdzhanova, G. Katsaros, K. Kern, T. H. Metzger, and O. G. Schmidt, Nano Lett. **8**, 1404 (2008).
[16] M. Stoffel, A. Malachias, T. Merdzhanova1, F. Cavallo, G. Isella, D. Chrastina, H. von Känel, A. Rastelli, and O. G. Schmidt, Semicond. Sci. Technol. **23**, 085021 (2008).
[17] M. A. Lutz, R. M. Feenstra, P. M. Mooney, J. Tersoff, and I. O. Chu, Surf. Sci. **316**, L1075 (1994).
[18] Z. Zhong, W. Schwinger, F. Schäffler, G. Bauer, G. Vastola, F. Montalenti, and L. Miglio, Phys. Rev. Lett. **98**, 176102 (2007).
[19] G. Katsaros, J. Tersoff, M. Stoffel, A. Rastelli, P. Acosta-Diaz, G. S. Kar, G. Costantini, O. G. Schmidt, and K. Kern, Phys. Rev. Lett. **101**, 096103 (2008).
[20] H. Hu, H. J. Gao, and F. Liu, Phys. Rev. Lett. **101**, 216102 (2008).
[21] A. Malachias, S. Kycia, G. Medeiros-Ribeiro, R. Magalhães-Paniago, T. I. Kamins, and R. Stanley Williams, Phys. Rev. Lett. **91**, 176101 (2003).
[22] T. U. Schülli, G. Vastola, M.-I. Richard, A. Malachias, G. Renaud, F. Uhlík, F. Montalenti, G. Chen, L. Miglio, F. Schäffler, and G. Bauer, Phys. Rev. Lett. **102**, 025502 (2009).
[23] G. Medeiros-Ribeiro and R. Stanley Williams, Nano Lett. **7**, 223 (2007).
[24] M. S. Leite, G. Medeiros-Ribeiro, T. I. Kamins, and R. Stanley Williams, Phys. Rev. Lett. **98**, 165901 (2007).